A Metal Oxide Memristor-Based Oscillators and Filters

Stoyan M. Kirilov, Ivan D. Zaykov

***Abstract* — Memristors are novel and nano-sized electronic passive elements with memorizing properties, potentially applicable in different electronic schemes, as neural networks, memory circuits, analog and digital devices, which design requires precise and simple models. In this paper, a modified and improved model of metal oxide memristors is proposed, in order to be used for preliminary engineering of memristor-based generators, filters and other electronic circuits. The offered model has a high accuracy, simplified math expressions and includes activation thresholds as well. Its corresponding LTSPICE library model is generated and applied for analysis of oscillators, low-pass and high-pass filters. The suggested model correctly expresses the nonlinear ionic dopant drift. The basic current-voltage and state-flux relationships are analyzed for both soft-switching and hard-switching modes. The conducted analyses and simulations confirm its correct operation in electronic circuits, representing the main fingerprints of memristor elements.**

***Index Terms* — metal oxide memristors, nonlinear ionic dopant drift, activation thresholds, LTSPICE library model**

I. INTRODUCTION

In the last fifteen years, resistance switching effects in transition metal oxide compounds have been intensively analyzed [1, 2]. They are mainly related to the variation of the oxide material's resistance according to the applied voltage and the stored electric charges [2]. These metal oxides could remember their conductance for a long-time interval after switching the electric sources off [3]. They collect charges, which amount is proportional to the time integral of the electric current [4]. Due to these useful memorizing properties, transition metal oxides as TiO_2, HfO_2, Ta_2O_5, NbO and others could be potentially used as storing components in memory schemes [4-6]. The existence of the fourth basic two-terminal passive nonlinear element – the memristor, is forecasted by Leon Chua in 1971 [7]. In 2008 the first material memristor based on TiO_2 is invented by a Hewlett-Packard research group headed by Stanley Williams [8]. After this important discovery, many scientific and technical teams tried to create memristive elements, based on different materials and fabrication technologies [9, 10]. Some different types of memristive elements, made of organic and polymeric materials, spintronic and magnetic physical structures [11], amorphous silicon dioxide [12] and others are reported in the scientific papers [13]. Several of the main respected memristors' properties are their established non-volatility, memory effect, lower energy consumption, high switching rate, very good compatibility to the present CMOS integrated circuits technologies, and their nano-sized dimensions [14-16]. These useful properties are related to the possible applications of memristors in memory devices and circuits [17, 18], programmable analog and digital electronic schemes, artificial neural networks and others [19, 20]. The engineering of electronic devices and circuits requires their preliminary analysis by computer-based simulations [21-23]. Among the other widely spread software environments for electronic circuits' simulations, as OrCAD PSPICE, HSPICE, and Microsim, LTSPICE is a very appropriate one for scientific research because it is a simplified, user-friendly, and free of charge software [24, 25]. Some specialized models for TiO_2, HfO_2, and Ta_2O_5 memristive elements are reported in the technical papers [26-29]. Owing to some specifics of their physical structure, operation and behavior in electric field, such memristive elements are quite different to each other [30-32]. Nevertheless, in many cases generalized models could be used for a broad class of transition metal oxide-based memristors. The specific and precise models for metal oxide-based memristive elements at times are relatively complex for SPICE incorporation [24]. The basic purpose of this work is to suggest a simplified, fast-functioning and general LTSPICE memristor model with a high accuracy, appropriate for analysis and computer simulations of different types transition metal-oxide memristors. The offered simple and enhanced memristor model is mainly based on Lehtonen-Laiho model [27]. Its main advantages, with respect to many of the existing and standard memristor models, are the simplified math relationships, good correctness and fast functioning in simulation software environments. Another advantage of the proposed model is the use of activation (sensitivity) thresholds, which ensure its applicability in artificial neural networks, memory devices and reconfigurable electronic schemes [30, 31]. The offered memristive model is included and analyzed in simple analog filters and oscillators [33, 34]. After a comparison to experimental *i-v* relationships [5, 6,19] and to results obtained by several of the mainly applied memristor models [26, 27], it is established that the considered model has a high accuracy. For restriction the state variable and expression the boundary effects for hard-switching mode, an enhanced Biolek window [24, 31] is used. For avoidance of convergence issues, a modified and differentiable sigmoid step-like function is applied in the

This paper is submitted on 11.04.2022 after review.

S. M. Kirilov is with the Department Fundamentals of Electrical Engineering, Technical University of Sofia, 1000 Sofia, Bulgaria (e-mail: s_kirilov@tu-sofia.bg).

I. D. Zaykov is with the Department Fundamentals of Electrical Engineering, Technical University of Sofia, 1000 Sofia, Bulgaria (e-mail: ivanzaykov@tu-sofia.bg).

https://doi.org/10.47978/TUS.2022.72.02.006

corresponding LTSPICE memristor model.

The rest of the present paper is organized as follows. Section 2 represents a brief description of the main transition metal oxide-based memristor elements and their modeling. The suggested general memristor model is presented in Section 3. The respective LTSPICE memristor library model is explained in Section 4. Its application and operation in oscillators and filters are discussed in Section 5. The conclusion of the work is presented in Section 6.

II. A Brief Description of Memristor Modeling

For better understanding and summary of memristor functional operation and modeling, a brief explanation of the fundamentals of metal-oxide memristors is presented. A simplified structure of metal-oxide memristor is presented in Fig. 1 for further explanations. The metal-oxide memristor has two terminals – *anode* and *cathode* [19]. The doped region is saturated by oxygen vacancies, generated by electroforming process [8]. For Ta_2O_5 memristive elements the state variable is the ratio between the surfaces of the central region a_1 and those of the entire memristor cross-section a_2 [6]. The *state variable x* of titanium dioxide and *hafnium dioxide* memristive components is represented as a ratio between the sizes of the doped layer *w* and those of the whole element *D* [8].

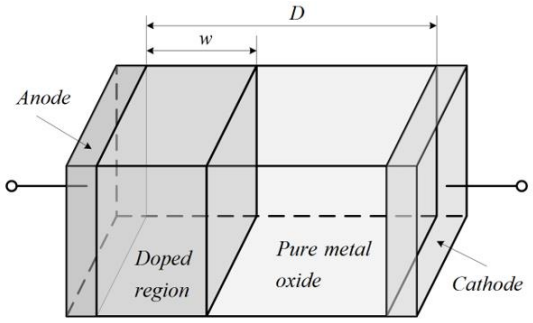

Fig. 1. A physical structure of transition metal oxide-based memristor

The state variable of a metal-oxide memristor *x* then might be expressed by (1) [8, 31, 32]:

$$x = D^{-1} \cdot w, \quad 0 \le x \le 1 \tag{1}$$

The state-dependent relation between the voltage across the memristor nanostructure *v* and the respective current of the element *i* is [8]:

$$v = i \cdot M = i \cdot \left[R_{OFF} \left(1 - x\right) + R_{ON} x \right] \tag{2}$$

Here, equation (2) is expressed according to Strukov-Williams memristor model [8], R_{ON} and R_{OFF} are the ON-state and OFF-state resistances and *M* is the memristor's resistance, also known as a *memristance* [8]. The equations that fully represent a memristor behavior include the *state differential relation*, connecting the time derivative of the state variable *x* and the current, and the state-dependent *current-voltage relationship* [30]:

$$\begin{cases} \dfrac{dx}{dt} = k \cdot f\left(x,i\right) \cdot i \\ v = M \cdot i \end{cases} \tag{3}$$

where *f(x,i)* is a window function used for restriction of the memristor state variable *x* in the range [0,1] and for expression of the related border effects, and *k* is a constant, associated to the physical properties of the memristive element – the ionic drift mobility μ, the ON-state resistance R_{ON} and length of the memristor element *D* [8]:

$$k = \mu \frac{R_{ON}}{D^2} \tag{4}$$

The *mobility* of the electric charges μ depends on the applied voltage. It rises exponentially when the electric field intensity *E* is higher than a threshold value [4]. The respective physical processes associated to this effect are complex and not accurately representable by a simplified model. The Lehtonen-Laiho model is commonly applied for investigation of metal oxide-based memristive elements [27]. It is with a high precision and properly describes the nonlinear drift of the oxygen vacancies. This memristor model is represented by the next equations' set [27]:

$$\begin{cases} i = x^n \cdot \beta \cdot \sinh\left(\alpha v\right) + \chi\left[\exp\left(\gamma v\right) - 1\right] \\ \dfrac{dx}{dt} = a \cdot f_B\left(x,i\right) \cdot v^m \end{cases} \tag{5}$$

where β, α, γ, χ, *a*, *n*, and *m* and are parameters for fine-adjustment of the model [27]. The first term in (5) expresses the dependence of the current on the applied voltage and the state variable, while the second one represents its rapid increase with the voltage [27]. For simplification of the suggested model, an approximation of the *exponential ionic drift* [4, 27] is presented in the next section.

III. The Suggested Memristor Model

The offered memristor model is fully expressed by equation (6). The coefficients k_1, k_2, k_3 and k_4 are used for tuning of the memristor model.

$$\begin{cases} i = \left(k_1 v^5 + k_2 v\right) x^5 \\ \dfrac{dx}{dt} = 0, \quad \left|v\right| < v_{thr} \\ \dfrac{dx}{dt} = k_3 \left(k_4 v\right)^3 f_{BM}\left(x,i\right), \quad \left|v\right| \ge v_{thr} \end{cases} \tag{6}$$

The first equation is a simplified version of the corresponding expression in the Lehtonen-Laiho model [27] and represents the relationship between the memristor voltage *v* and the current *i*. The second expression in (6) includes the *activation threshold* v_{thr}, and according to this equation the memristor state variable *x* has a constant value when the applied voltage is lower than this threshold. The third equation in (6) represents the time derivative of the memristor state variable *x* as a function of the applied voltage *v*. When the absolute value of the voltage is lower than the *sensitivity threshold* v_{thr}, then the memristive element operates as a simple linear resistor [30, 31]. When the signal's level exceeds the *activation threshold* v_{thr}, then the variation of the state variable is proportional to the applied voltage. The term $k_3(k_4.v)^3$ is applied in the final

equation of (6) for approximate representation of the nonlinear ionic dopant drift. The included in (6) modified *Biolek window function* $f_{BM}(x,i)$, which is founded on the smooth and differentiable sigmoidal function *stpp(i)* is presented by the next equations (7) [24, 31]:

$$f_{BM}(x,i) = 1 - \left[x - stpp(-i)\right]^{2p}$$
$$stpp(i) = \frac{1}{2}\cdot\left[\left(i^2+s\right)^{-0.5} i + 1\right] \quad (7)$$

The improved window f_{BM} [31] is a better form of the traditional Biolek window function [26]. It includes the step-like *sigmoid function stpp(i)*, as an alternative of the standard *Heaviside function*. This replacement leads to avoidance of convergence problems in SPICE. The rapid change of the sigmoidal function in the switching range depends on the parameter *s*, which is involved in the second expression. Its value is in the range [0.001, 1.10^{-5}] [24, 30]. The proposed memristor model is tested by sinusoidal voltage for both hard-switching and soft-switching functional modes. The optimal values of the model's parameters are obtained by parameter estimation, applying gradient descent of the root mean square (RMS) error between the simulated and experimental currents and simulation annealing [30, 31]. The derived values of the parameters are: k_1 = 0.11, k_2 = 0.13, k_3=803.2, k_4=1.52, m = $1.03.10^{-7}$, x_0 = 0.3, v_{thr} = 0.1, p = 10. The time diagrams of the voltage, state variable and current, according to the suggested model, Lehtonen-Laiho memristor model, Biolek and Joglekar models are illustrated in Fig. 2 for comparison and proving of the model's proper operation. The model's behavior in this case is similar and it corresponds to a soft-switching mode, because the state variable is altering in the interval (0.4, 0.7). The current has a highly non-sinusoidal form, due to the nonlinearity of the memristor models. The graphs, related to Joglekar and Biolek's models almost coincide one to another.

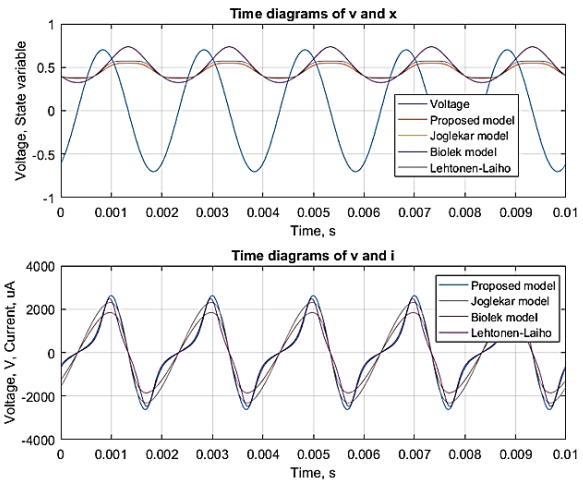

Fig. 2 Time diagrams of the applied voltage, state variable and the corresponding currents according to the suggested memristor model, Lehtonen-Laiho model, Joglekar and Biolek memristor models

The corresponding current-voltage and state-flux relationships are shown in Fig. 3 for expression of the correct operation of the proposed memristor model. The *i-v* relations are pinched hysteresis loops and the respective state-flux characteristics are single-valued ones, and this confirms the operation in a soft-switching mode. The characteristics, related to Biolek and Joglekar models in this case almost match to each other.

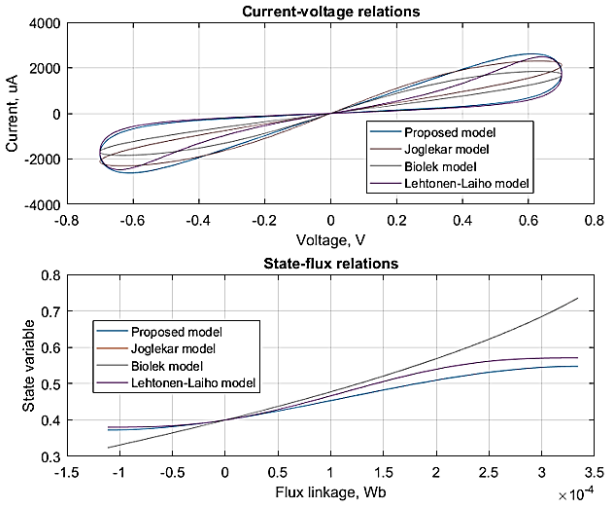

Fig. 3. Current-voltage and state-flux relationships, derived by the proposed model, Lehtonen-Laiho memristor model, Biolek and Joglekar models

The simulation time of the suggested model is about 17.3 ms, for Lehtonen-Laiho model it is about 16.9 ms, for Biolek model – 16.4 ms, and for Joglekar model – 16.1 ms. The respective RMS errors are: 2.71 % for the suggested model, 2.63 % for Lehtonen-Laiho model, 3.46 % for Biolek model, and for Joglekar model – 3.71 %. It could be stated that rendering to the simulation times and errors, the offered memristor model has a good precision, near to Lehtonen-Laiho model, and it has lesser simulation time.

Using expressions (6) and (7) and the model's parameters, the LTSPICE memristor model is generated and considered in the next section.

IV. The Corresponding LTSPICE Model

Via the offered memristor model, expressed by (6) and (7), a corresponding LTSPICE [17, 18] memristor model is created. The basic elements in the LTSPICE software [21] are applied for the mathematical expressions, rendering to the considered memristor model.

The respective circuit of the LTSPICE metal-oxide memristor model is given in Fig. 4 for additional explanations. The memristor state variable x is related to the voltage $V(Y)$ across the capacitor C_1 [31]. The current of the capacitive element is correspondent to the time derivative of x. The voltage-dependent current source G_1 expresses the memristor current. The resistor R_1, attached in parallel to C_1 keeps the considered model from convergence problems [30]. The terminals of the memristor are the anode (a) and the cathode (c). The electrode Y is used for measuring the state variable x.

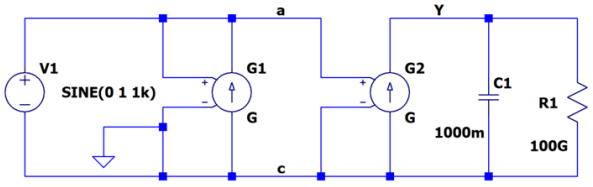

Fig. 4. LTSPICE schematic of the proposed memristor model B_{14}

Based on the corresponding schematic, LTSPICE code of the metal oxide-based memristor model is derived and shown as follows.

```
.subckt B14 a c Y
.params k1=0.11 k2=0.13 k3=803.2 k4=1.52
.params m=1.3e-7 vthr=0.1 pp=10
Cint Y 0 1 IC=0.3
Rad Y 0 100G
Gy 0 Y value={k3*pow((k4*V(a,c)),3)*
(1-pow((V(Y)-stpp(-V(a,c),m)),(2*pp)))*
(stpp((abs(V(a,c))-vthr),m))}
G1 a c value={(k1*pow(V(a,c),5)+k2*
V(a,c))*pow(V(Y),5)}
.func stpp(x,p)={0.5*(1+(x/sqrt(pow(x,2)+p)))}
.ends B14
```

The proposed LTSPICE model is investigated under impulse operation and by sinusoidal signals with different frequencies. The memristor library model, denoted by B_{14} is involved in a simple electric circuit for testing of its operation and behavior. It is shown in Fig. 5 for depiction of its basic components and connections. The terminal Y is attached to a high-valued resistor R_1, preventing the alteration of the state. The dependent source B_1 is used for obtaining a signal, proportional to the flux linkage.

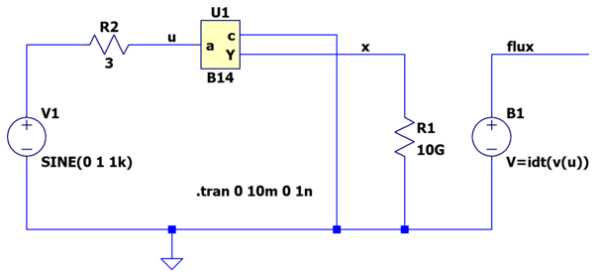

Fig. 5. A circuit for testing of the suggested model, including a voltage source V_1 and integrator B_1 for deriving the flux linkage

The obtained voltage-current relationships are presented in Fig. 6 for validation of the accurate operation of the model. It is obvious that, if the frequency of the signal rises, then the area of the current-voltage loops decreases. This effect is in agreement with the fundamental fingerprints of the memristor components [8, 30].

The memristive model is also analyzed under pulse regime, representing both hard-switching and soft-switching modes. Rendering to Lehtonen-Laiho model [27], the suggested here memristor model is with a lesser simulation time. The correctness of the suggested memristor model is near to those of Lehtonen-Laiho model, according to the derived RMS error. According to Biolek and Joglekar models, the proposed one has a little bit higher simulation time and higher precision.

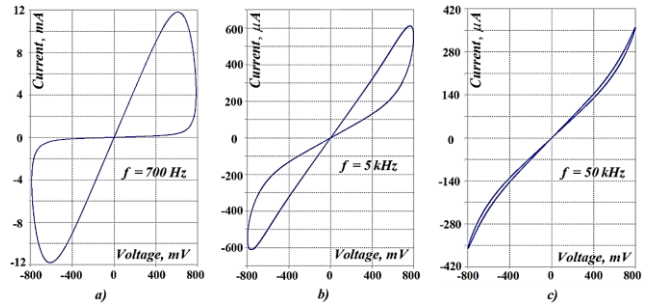

Fig. 6. Current-voltage relationships, obtained by the proposed model at different frequencies a) f = 700 Hz; b) f = 5 kHz; c) f = 50 kHz

V. Memristor-Based Generator and Filters

5.1. A memristor-based oscillator scheme

The explained in this section memristor-based oscillator is presented in Fig. 7. It is based on resistor-capacitor circuits for phase-shifting [33, 34], where the resistors are replaced by memristor elements. The circuit contains an operational amplifier, denoted by U_1. The voltage sources V_1 and V_2 are used for its power supply. The capacitors are previously charged and their initial voltage is about 0.1 V. The capacitances are with a value of 100 nF. The included memristors are denoted by U_2 – U_5. The final memristor is used for adjustment of the output signal, presented in Fig. 8. It is visible that the generated output signal has a sinusoidal form and the transient has a duration about 2.1 ms. The frequency of the generated output signal is about 1 kHz. The frequency of the generated signal is tuned by the change of the memristances of U_2, U_3 and U_4.

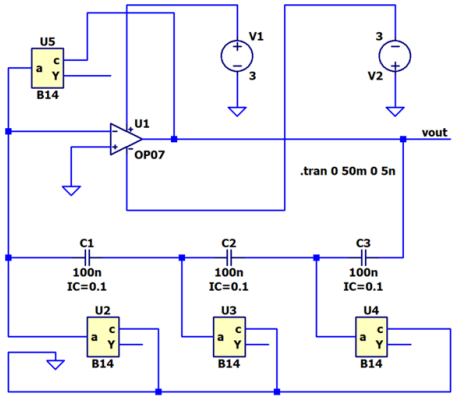

Fig. 7. A memristor-based generator with operational amplifier and capacitive elements

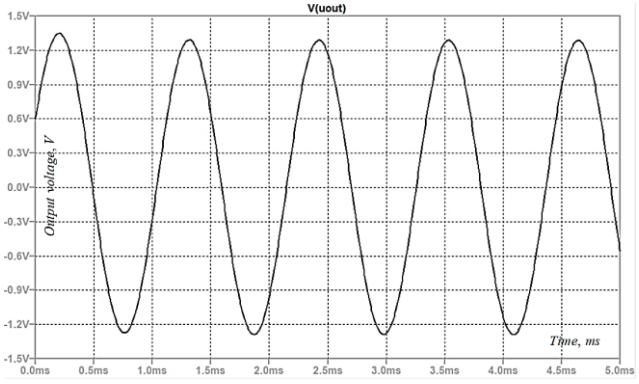

Fig. 8 Time diagram of the output voltage of the memristor oscillator

5.2. Memristor-based analog low-pass and high-pass filtering groups

The described below analog filtering circuits are presented in Fig. 9 for further clarification of their operation and basic properties. In the following schemes of low-pass and high-pass filters, the use of inductances is avoided, applying only resistors (memristors) and capacitors [33]. In the normal operating mode, the memristors behave as linear resistors. Their tuning is realized by external voltage pulses and the change of their resistance leads to alteration of the cut-off frequencies and the pass-bands.

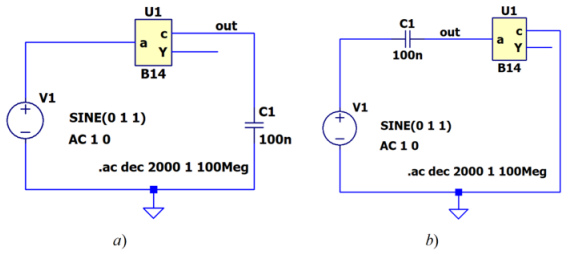

Fig. 9 Schematics of a low-pass filter (a) and a high-pass filter (b)

The amplitude-frequency and phase-frequency responses of the memristor-based filters are presented in Fig. 10 for better description of their properties and operation. The resistances of the memristors U_1 and U_2 are changed by external signals, which are not depicted in the presented circuits. In this way, the cut-off frequencies of the filters could be changed, related to the alteration of the memristance and the corresponding state variable [14]. The load resistances of the analog filters are very high-valued. The cut-off frequencies are about 12 kHz and the corresponding state variable is x = 0.42. The respective memristance is M = 7.2 kΩ.

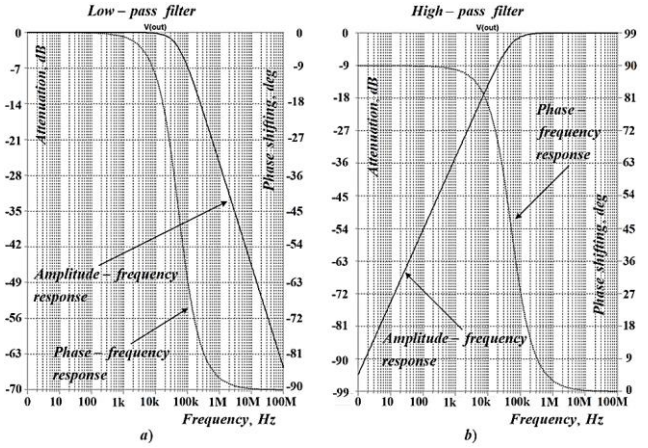

Fig. 10. Amplitude-frequency and phase-frequency responses of the low-pass filter (a) and the high-pass filter (b)

The low-pass filtering group has a cut-off frequency, which is dependent on the resistance of the memristor element M and the capacitance C_1 [33, 34]:

$$f_{cut-off\ low} = \frac{1}{2\pi M_1 C_1} \tag{8}$$

The corresponding cut-off frequency of the high-pass filtering module is presented as follows [33, 34]:

$$f_{high\,cut-off} = \frac{1}{2\pi M_2 C_2} \tag{9}$$

The cut-off frequencies could be adjusted by altering the memristances and the correspondent state variables by external voltage or current pulses [14, 31]. It could be denoted that in the considered memristor-based oscillator and filters, the memristor elements operate with low-level signals, which are with amplitude lesser than the sensitivity thresholds. Owing to this, their behavior is identical to those of their classical resistive analogs. Additional simulations and analyses confirm their similarity and proper operation.

VI. Conclusion

In this work, a modified and improved metal oxide-based memristor model is suggested. It is based on the classical Lehtonen-Laiho model and a tantalum memristor model, with a simplified and highly nonlinear relation between the time derivative of the state variable and the applied voltage. The increased nonlinearity allows to the presented memristor model to correctly operate at high-frequency signals. Founded on the presented metal oxide memristive model, oscillator and filtering schemes are analyzed. Their operation is presented, paying attention on the main advantages, with respect to the traditional capacitor-resistor alternatives. The proper functioning of the considered memristor model is confirmed by comparison with several of the widely used models, as Joglekar, Biolek and Lehtonen-Laiho models.

The use of sensitivity thresholds allows the presented modified memristor model to be successfully included in adjustable memristor-based electronic circuits, as oscillators and analog filters. In the normal operating regime of these devices, when the voltage across the memristors is lower than the activation threshold, then the conductance of the memristive component is a constant and the filters operate as linear devices. For changing the cut-off frequencies and the respective pass-bands, externally applied to the memristors voltage pulses are used. For higher-frequency signals, Joglekar and Biolek memristor models are suitable for inclusion in such electronic circuit, but the suggested model has a better performance, according to the linearity of the filtering circuits, owing to the use of sensitivity thresholds.

References

[1] Chiu, F.C., „A Review on Conduction Mechanisms in Dielectric Films,“ In Advanced Materials Science Engineering; Hindawi Publishing Corporation: London, UK, 2014, Vol. 2014, pp. 1–18, https://doi.org/10.1155/2014/578168

[2] Mohammad, B., Jaoude, M., Kumar, V., Al Homouz, D., Nahla, Heba Abu, Al-Qutayri, M., Christoforou, N., "State of the art of metal oxide memristor devices," Nanotech. Rev., vol. 5, no. 3, 2016, pp. 311-329, https://doi.org/10.1515/ntrev-2015-0029

[3] Dearnaley, G., Stoneham, A. M., Morgan, D. V., “Electrical phenomena in amorphous oxide films,” Rep. Prog. Phys. 1970, 33, pp. 1129–1191, https://doi.org/10.1088/0034-4885/33/3/306

[4] Strukov, D. B., Williams, S., “Exponential ionic drift: Fast switching and low volatility of thin-film memristors,” Applied Physics A 2009, pp. 515–519, https://doi.org/10.1007/s00339-008-4975-3

[5] Amer, S., Sayyaparaju, S., Rose, G., S, Beckmann, K., Cady, N.C., “A practical hafnium-oxide memristor model suitable for circuit design and simulation,” In 2017 IEEE (ISCAS) 2017 May 28, pp. 1-4, DOI: 10.1109/TCT.1971.1083337.

[6] Strachan, J., Torrezan, A., Miao, F., Pickett, M., Yang, J., Yi, W., Medeiros-Ribeiro, G., Williams, R. S., “State Dynamics and Modeling of Tantalum Oxide Memristors,” IEEE Transactions on Electron Devices, 2013, pp. 2194–2202, https://doi.org/10.1109/TED.2013.2264476

[7] Chua, L. “Memristor-The missing circuit element,” IEEE Trans. Circuit Theory 1971, 18, pp. 507–519, https://doi.org/10.1109/TCT.1971.1083337

[8] Strukov, D. B., Snider, G. S., Stewart, D. R., Williams, S. “The missing memristor found,” Nature 2008, 453, pp. 80–83, https://doi.org/10.1038/nature06932

[9] Mladenov, V., "A Modified Tantalum Oxide Memristor Model for Neural Networks with Memristor-Based Synapses," 2020 9th International Conference on Modern Circuits and Systems Technologies (MOCAST), 2020, pp. 1-4, doi: 10.1109/MOCAST49295.2020.9200238.

[10] Mladenov, V., “Analysis of Memory Matrices with HfO_2 Memristors in a PSpice Environment,” MDPI Electronics 2019, 8(4), 383. https://doi.org/10.3390/electronics8040383.

[11] McConville, J.P., Lu, H., Wang, B., Tan, Y., Cochard, C., Conroy, M., Moore, K., Harvey, A., Bangert, U., Chen, L.Q. and Gruverman, A., 2020. "Ferroelectric domain wall memristor," Advanced functional materials, 30(28), p.2000109, https://doi.org/10.1002/adfm.202000109

[12] Jaafar A. H. et al., "Evidence of Nanoparticle Migration in Polymeric Hybrid Memristor Devices," 2020 European Conference on Circuit Theory and Design (ECCTD), 2020, pp. 1 - 4, doi: 10.1109/ECCTD49232.2020.9218360.

[13] Park, H. L., Kim, M. H. and Lee, S. H., "Control of conductive filament growth in flexible organic memristor by polymer alignment. Organic Electronics," 2020, 87, p.105927, https://doi.org/10.1016/j.orgel.2020.105927

[14] Mladenov, V. "Advanced Memristor Modeling—Memristor Circuits and Networks," MDPI: Basel, Switzerland, 2019; p. 172. ISBN 978-3-03897-104-7 (Hbk).

[15] Wang, X., Chen, Y., Xi, H., Li, H., Dimitrov, D., "Spintronic Memristor Through Spin-Torque-Induced Magnetization Motion," IEEE Electron Device Lett. 2009, 30, pp. 294–297, https://doi.org/10.1109/LED.2008.2012270

[16] Chen, Y., Liu, G., Wang, C., Zhang, W., Li, R.-W., Wang, L., "Polymer memristor for information storage and neuromorphic applications," Mater. Horizons 2014, 1, pp. 489–506, https://doi.org/10.1039/C4MH00067F

[17] Mladenov, V., "A New Simplified Model for HfO2-Based Memristor," 2019 8th International Conference on Modern Circuits and Systems Technologies (MOCAST), 2019, pp. 1-4, doi: 10.1109/MOCAST.2019.8741953.

[18] Li, C., Hu, M., Li, Y. et al., "Analogue signal and image processing with large memristor crossbars," Nat. Electron. 1, 52–59 (2018). https://doi.org/10.1038/s41928-017-0002-z.

[19] Mbarek, K., Rziga, F. O., Ghedira, S., Besbes, K., "An analysis of the dynamics of SPICE memristor model," 2017 (ICCAD), 2017, pp. 054-059, doi: 10.1109/CADIAG.2017.8075630.

[20] Mladenov, V., "A New Simplified Model and Parameter Estimations for a HfO2-Based Memristor," †. Technologies, 2020; 8(1):16. https://doi.org/10.3390/technologies8010016.

[21] May, C. "Passive Circuit Analysis with LTspice® - An Interactive Approach," Springer Nature Switzerland AG 2020, ISBN 978-3-030-38304-6, https://doi.org/10.1007/978-3-030-38304-6, pp. 763.

[22] Solovyeva, E. B., Azarov, V. A., "Comparative Analysis of Memristor Models with a Window Function Described in LTspice," 2021 IEEE Conference of Russian Young Researchers in Electrical and Electronic Engineering (ElConRus), 2021, pp. 1097-1101, doi: 10.1109/ElConRus51938.2021.9396217.

[23] Yang, W. Y., Cao, W., Chung, Tae-Sang, Morris, J., "Applied numerical methods using MATLAB," John Wiley & Sons, Inc., ISBN 0-471-69833-4, 2020, pp. 509.

[24] Mladenov, V., "A Unified and Open LTSPICE Memristor Model Library," MDPI Electronics, 2021, Vol. 10, no. 13, 1594. https://doi.org/10.3390/electronics10131594, pp. 1 – 27.

[25] Linn, E., Siemon, A., Waser, R., Menzel, S., "Applicability of Well-Established Memristive Models for Simulations of Resistive Switching Devices," IEEE Trans. Circuits Syst. 2014, 61, pp. 2402–2410, https://doi.org/10.1109/TCSI.2014.2332261

[26] Biolek, Z., Biolek, D., Biolkova, V., "SPICE Model of Memristor with Nonlinear Dopant Drift," Radioengineering 2009, 18, pp. 210–214.

[27] Lehtonen, E., Laiho, M., "CNN using memristors for neighborhood connections", In Proceedings of the 2010 12th (CNNA 2010), Berkeley, CA, USA, 3–5 February 2010, pp. 1–4, https://doi.org/10.1109/CNNA.2010.5430304

[28] Joglekar, Y., Wolf, S. J., "The elusive memristor: Properties of basic electrical circuits," Eur. J. Phys. 2009, 30, pp. 661–675, https://doi.org/10.1088/0143-0807/30/4/001

[29] Mladenov, V. "Analysis and Simulations of Hybrid Memory Scheme Based on Memristors," MDPI Electronics, 2018; 7(11):289. https://doi.org/10.3390/electronics7110289.

[30] Ascoli, A., Tetzlaff, R., Biolek, Z., Kolka, Z., Biolkova, V., Biolek, D., "The Art of Finding Accurate Memristor Model Solutions," IEEE J. Emerg. Sel. Top. Circuits Syst. 2015, 5, pp. 133–142, https://doi.org/10.1109/JETCAS.2015.2426493

[31] Ascoli, A., Corinto, F., Senger, V., Tetzlaff, R., "Memristor Model Comparison," IEEE Circuits Syst. Mag. 2013, 13, pp. 89–105, https://doi.org/10.1109/MCAS.2013.2256272

[32] Mladenov, V., "Synthesis and Analysis of a Memristor-Based Artificial Neuron," CNNA 2018; The 16th International Workshop on Cellular Nanoscale Networks and their Applications, pp. 1-4.

[33] Winder, S., "Analog and digital filter design," 2002, Elsevier Science, USA, ISBN 0-7506-7547-0.

[34] Lautaro Fernandez-Canque, H., "Analog Electronics Applications – fundamentals of design and analysis," CRC Press Taylor & Francis Group, ISBN 978-1-4987-1495-2, 2017.